International Journal of Thermal Sciences 49 (2010) 580–588

Contents lists available at ScienceDirect

International Journal of Thermal Sciences

journal homepage: www.elsevier.com/locate/ijts

Finned tube performance evaluation with nanofluids and conventional heat transfer fluids

Roy Strandberg, Debendra K. Das*

Department of Mechanical Engineering, University of Alaska Fairbanks, P.O. Box 755905, Fairbanks, AK 99775-5905, USA

ARTICLE INFO

Article history:
Received 21 May 2009
Received in revised form
24 July 2009
Accepted 31 August 2009
Available online 6 October 2009

Keywords:
Nanofluids
Ethylene glycol
Finned tube
Heating capacity
Natural convection
Particle concentration
Hydronic system
Temperature dependency

ABSTRACT

The performance of hydronic finned-tube heating units with nanofluids is compared to their performance with a conventional heat transfer fluid comprised of 60% ethylene glycol and 40% water, by mass (60% EG) using a mathematical model. The nanofluids modeled are comprised of either CuO or Al_2O_3 nanoparticles dispersed in the 60% EG solution. The finned tube configuration modeled is similar to that commonly found in building heating systems. The model employs correlations for nanoparticle thermophysical properties and heat transfer that have been previously documented in the literature. The analyses indicate that finned tube heating performance is enhanced by employing nanofluids as a heat transfer medium. The model predicts an 11.6% increase in finned-tube heating output under certain conditions with the 4% Al_2O_3/60% EG nanofluid and an 8.7% increase with the 4% CuO/60% EG nanofluid compared to heating output with the base fluid. The model predicts that pumping power required for a given heating output with a given finned tube geometry is reduced with both the Al_2O_3/60% EG and the CuO/60% EG nanofluids compared to the base fluid. The finned tube with 4% Al_2O_3/60% EG has the lowest liquid pumping power at a given heating output of all the fluids modeled.

© 2009 Elsevier Masson SAS. All rights reserved.

1. Introduction

Heat transfer fluids that are enhanced with extremely small particles (less than 100 nm in their characteristic dimension, often called "nanoparticles") in dispersion, are often referred to as "nanofluids". These fluids have been shown in studies by multiple authors to exhibit superior thermal conductivity [4] to that predicted by conventional correlations developed for fluids enhanced with micrometer-sized particles. Other studies have focused on developing correlations to predict the Nusselt number of internal flows for nanofluids. For example, the work of Li and Xuan [8], Xuan and Li [18], suggests that Nusselt numbers for nanofluids are superior to those of the base fluid under certain flow conditions (for instance, when directly compared at equal Reynolds numbers). The higher Nusselt numbers, combined with higher thermal conductivity yields superior convective heat transfer compared to conventional heat transfer fluids coefficients in internal flow situations. The dispersion of the nanoparticles into fluids also results in higher viscosity that is related to particle mean diameter, concentration and temperature. Under certain flow conditions (for constant average liquid velocity, for instance), this can result in increased pumping losses. The higher viscosity also contributes to a reduction in Reynolds number, which decreases the Nusselt number when compared to conventional fluids under constant velocity conditions. These factors must be weighed against each other in evaluating the suitability of nanofluids for use in heat transfer applications.

Finned tube radiators are often used to provide comfort heating in perimeter zones within occupied spaces of buildings. These finned tubes are comprised of a copper tube or steel pipe with thin, rectangular fins mechanically crimped onto the outside diameter at regular intervals. Heat transfer fluid is pumped through the copper tubing while room air is drawn over the fins by natural convection, thereby accomplishing heat transfer between the hot heating fluid and the cooler room air. The application of nanofluids in these finned tube radiators may result in several potential benefits including increased heating output for equal liquid flow. These performance impacts, in turn, may be translated into a reduction in total required heat transfer area. This trait can used to reduce the materials of construction needed to achieve a given rate of the heating output. Superior heat transfer properties of nanofluids may also result in lower liquid flow rate for a given rate of heat transfer, yielding a reduction in the liquid pumping power consumed compared to the base fluid.

The objective of this work is to characterize the performance of finned tube radiators with CuO/60% EG and Al_2O_3/60% EG nanofluids

* Corresponding author. Tel.: +1 907 474 6094; fax: +1 907 474 6141.
E-mail address: dkdas@alaska.edu (D.K. Das).

1290-0729/$ – see front matter © 2009 Elsevier Masson SAS. All rights reserved.
doi:10.1016/j.ijthermalsci.2009.08.008

at different volumetric concentrations, and to compare the finned tube radiators' performance to that with the 60% EG base fluid. In cold regions of the world such as Alaska, 60% EG is employed as a heat transfer fluid because of its extreme freeze resistance. Heating output for a given finned tube geometry is characterized using the nanofluids and the base fluid. Also characterized are frictional pressure loss, pumping power and heat transfer area associated with a given heating output using the nanofluids and the base fluid.

2. Analysis

The methodology employed to determine finned-tube heating capacity was based on several previously developed correlations for thermophysical properties. Selected correlations for properties of the air and the 60% ethylene glycol/water solution were based on curve-fits generated from published property data.

2.1. Heat transfer fluid thermophysical properties

In this analysis, liquid filled finned-tube heating capacity is compared for a variety of different heat transfer fluids. These include 60% ethylene glycol/40% water solution (heretofore referred to as 60% EG) and nanofluids comprised of a 60% EG base fluid with CuO or Al_2O_3 nanoparticles uniformly dispersed in volumetric concentrations of 4% or less. Thermophysical property data for the 60% EG were taken from ASHRAE Fundamentals [1]. Thermophysical properties for air are taken from Bejan [2].

For all curve-fits applied to 60% EG property data (Eqs. (2), (8) and (11) below) and corresponding data for air (Eqs. (1), (7), and (10)), $R^2 > 0.99$. These correlations are applicable for 60% EG between 273 K $< T <$ 370 K, and for air between 173 K $< T <$ 333 K. These temperatures are comparable to those seen in facility heating systems.

2.1.1. Density

For density of air, a polynomial curve-fit was applied to the property data, with $R^2 > 0.99$. The equation for the fitted polynomial is

$$\rho_{\text{air}} = 2.3548 \times 10^{-5} \cdot T^2 - 1.7928 \times 10^{-2} \cdot T + 4.4289 \quad (1)$$

where ρ_{air} is in kg/m^3. For density of the 60% EG, a polynomial curve-fit was applied to the ASHRAE data. The equation for the fitted curve is

$$\rho_{bf} = -0.002475 \cdot T^2 + 0.9998 \cdot T + 1002.5023 \quad (2)$$

where ρ_{bf} is in kg/m^3. Pak and Cho [10] developed a relationship for the effective density of nanofluids. This is used for both types of nanofluids considered. It is stated as:

$$\rho_{nf} = \phi\rho_s + (1-\phi)\rho_{bf} \quad (3)$$

2.1.2. Specific heat

For specific heat of air, a constant value of 1006 J/kg K is used. For specific heat (J/kg K) of the 60% EG, a linear curve-fit was applied to the ASHRAE data. The equation for the fitted curve is:

$$c_{p,bf} = 4.248 \cdot T + 1882.4 \quad (4)$$

Buongiorno [3] has developed a relation for effective specific heat of nanofluids. Buongiorno's correlation is employed for evaluating the specific heat of CuO nanofluids. It is stated as:

$$c_{p,nf} = \frac{\phi\rho_s c_{p,s} + (1-\phi)\rho_{bf} c_{p,bf}}{\rho_{nf}} \quad (5)$$

From experiments on Al_2O_3 nanoparticles in 60% EG, Vajjha and Das [16] developed a specific heat correlation. It is stated as

$$\frac{c_{p,nf}}{c_{p,bf}} = \frac{\left((AT) + B\left(\frac{c_{p,s}}{c_{p,bf}}\right)\right)}{(C+\phi)} \quad (6)$$

where $A = 0.000891$, $B = 0.5179$ and $C = 0.4250$ and 315 K $< T <$ 363 K; $0.01 < \phi < 0.1$. Also, c_p is in kJ/(kg K).

2.1.3. Viscosity

For viscosity of air (in Pa s), a linear curve-fit was applied to the property data, with $R^2 > 0.99$. The equation for the fitted line is

$$\mu_{\text{air}} = 5.2638 \times 10^{-8} \cdot T + 2.6384 \times 10^{-6} \quad (7)$$

For viscosity of the 60% EG (in mPa s), a curve-fit based on Andrade's equation presented by Reid et al. [11] was applied to the ASHRAE data. The equation of this curve-fit is

$$\ln(\mu_{bf}) = 3135.6\left(\frac{1}{T}\right) - 8.9367 \quad (8)$$

This correlation applies for 273 K $< T <$ 360 K.Vajjha [14], developed the following correlations based on experimental data of Namburu et al. [9] for computing the viscosity (in mPa s) of nanofluids comprised of CuO and Al_2O_3 nanoparticles dispersed in 60% EG base fluid

$$\frac{\mu_{nf}}{\mu_{bf}} = Ae^{B\cdot\phi} \quad (9)$$

where $A = 0.9830$ and $B = 12.9590$ for Al_2O_3 with ϕ up to 10% ($0 < \phi < 0.10$) $A = 0.9197$ and $B = 22.8539$ for CuO with ϕ up to 6% ($0 < \phi < 0.06$).

This viscosity correlation was developed for 273 K $< T <$ 360 K.

2.1.4. Thermal conductivity

For thermal conductivity of air (W/m K), a linear curve-fit was applied to the property data, with $R^2 > 0.99$. The equation for the fitted line is

$$k_{\text{air}} = 7.5576 \times 10^{-5} \cdot T + 3.1203 \times 10^{-3} \quad (10)$$

For thermal conductivity of the 60% EG, a polynomial curve-fit was applied to the ASHRAE data. The equation of this curve-fit is

$$k_{bf} = -3.196 \times 10^{-6} \cdot T^2 + 2.512 \times 10^{-3} \cdot T - 0.10541 \quad (11)$$

From experiments on CuO and Al_2O_3 nanoparticles dispersed in 60% EG, Vajjha and Das [15] developed a thermal conductivity correlation based on an improvement of the Koo–Kleinstreuer [7] model.

$$k_{nf} = \left(\frac{k_s + 2k_{bf} - 2\phi(k_{bf} - k_s)}{k_s + 2k_{bf} + \phi(k_{bf} - k_s)}\right)k_{bf} + 5 \times 10^4 \beta\phi\rho_{bf} c_{p,bf}\sqrt{\frac{\kappa T}{\rho_s d_p}} f(T,\phi) \quad (12a)$$

where

$$f(T,\phi) = (2.8217 \times 10^{-2}\phi + 3.917 \times 10^{-3})(T/T_o) - (3.0669 \times 10^{-2}\phi + 3.91123 \times 10^{-3}).$$

For nanofluids comprised of Al_2O_3 nanoparticles,

$$\beta = 8.4407(100\phi)^{-1.07304} \quad (12b)$$

while for nanofluids comprised of CuO nanoparticles,

$$\beta = 9.881(100\phi)^{-0.9446} \tag{12c}$$

These correlations apply for 293 K $< T <$ 363 K. For Al_2O_3 $0.01 < \phi < 0.10$, while for CuO $0.01 < \phi < 0.06$. $T_o = 273$ K is the reference temperature.

The first term of Eq. (12a) is the well-known Hamilton–Crossers [6] equation, while the second term was developed to take into account the Brownian motion associated with the nanoparticles, that enhances the thermal conductivity of the fluid.

For this analysis, all of the thermophysical properties are evaluated for CuO and Al_2O_3 nanoparticles with diameters of 29 nm and 44 nm, respectively.

2.2. Fluid flow parameters

Reynolds number of the liquid flow through of the finned tube is computed using the equation

$$Re = \frac{\rho V d_i}{\mu} \tag{13}$$

On the airside of the finned tube, heat transfer is driven by natural convection. Correlations reported by Raithby and Hollands [13] are used to model this process. The Rayleigh number is computed with the relation

$$Ra = \frac{g\beta(T_w - T_\infty)s^3}{\nu\alpha}\frac{s}{D_E} \tag{14}$$

where $g\beta/\nu\alpha$ is computed using the following correlation:

$$\frac{g\beta}{\nu\alpha} = 1.0794 \times 10^{19} \cdot T^{-4.4626} \tag{15}$$

This correlation is based on property data of air from Bejan [2], for 223 K $< T <$ 1273 K, $R^2 > 0.99$.

The Nusselt number associated with the fin to air convective heat transfer is computed using the relation reported by Raithby and Hollands [13], originally developed for regularly spaced, round fins concentrically attached to a tube:

$$Nu_0 = \frac{Ra}{12\pi}\left\{2 - \exp\left[-\left(\frac{C_1}{Ra}\right)^{\frac{3}{4}}\right] - \exp\left[-\beta_1\left(\frac{C_1}{Ra}\right)^{\frac{3}{4}}\right]\right\} \tag{16}$$

where

$$\beta_1 = 0.17\zeta + e^{-4.8\zeta}, \quad \zeta = \frac{d_o}{D_E} \quad \text{and}$$

$$C_1 = \left[\frac{23.7 - 1.1(1 + 152\zeta^2)^{\frac{1}{2}}}{1 + \beta_1}\right]^{\frac{4}{3}} \tag{17}$$

The relation is adapted for use with a finned tube with rectangular fins by computing an equivalent diameter for the rectangular fins. This equation is:

$$D_E = 1.23(H) \tag{18}$$

For computing the convective heat transfer coefficient on the liquid side when the base fluid is circulating, a correlation developed by Gnielinski [5] from an extensive database for turbulent internal flows is selected.

$$Nu = 0.012(Re^{0.87} - 280)Pr^{0.4} \tag{19}$$

Gnielinski's correlation is valid for $1.5 \leq Pr$ 500 and $3 \times 10^3 \leq Re \leq 10^6$ and for liquids in a smooth, circular pipe, with fully developed flow.

For this study, Xuan and Li's [18] Nusselt number correlation for nanofluids was adopted.

$$Nu_{nf} = 0.0059(1.0 + 7.6286\phi^{0.6886}Pe_d^{0.001})Re_{nf}^{0.9238}Pr_{nf}^{0.4} \tag{20}$$

This is the only correlation available for nanofluids thus far that has been developed from experimental data on low concentration nanofluids ($\phi \leq 2\%$).

The inside convective heat transfer coefficient is computed using the standard relation:

$$h_i = \frac{Nu \cdot k}{d_i} \tag{21}$$

The following equation is employed to compute heat output from the finned tube section:

$$q_o'' = \frac{Nu_0 \cdot k(T_w - T_\infty)}{s} \tag{22}$$

and the total heat transfer rate is found using this equation:

$$q = q_o'' A_o \tag{22a}$$

On the liquid side, the following relation is used to compute heat transfer:

$$q = \dot{m}c_p(T_i - T_o) \tag{23}$$

For the purpose of the trial and error procedure for computing the finned-tube heating output described later, wall temperature is estimated using the equation:

$$T_w = T_m - \frac{q_o''}{h_i}\frac{A_o}{A_i} \tag{24}$$

For purposes of this analysis, the wall temperature is assumed to remain constant. Since the tubing is thin-walled copper, this assumption is reasonable. In determining heat transfer performance, fluid properties are evaluated at the bulk mean temperatures of the fluid streams.

2.3. Finned tube capacity calculation

To determine the output of the baseboard, a trial and error algorithm was developed. In the first step of the algorithm T_w is estimated. Based on this value, the airside Nusselt and Rayleigh numbers are computed. Then, using the airside Nusselt number, and considering the ambient temperature, the heating output from the finned tube is computed. Next, the fluid side outlet temperature is found using Eq. (23), where ρ, and c_p are evaluated at the liquid inlet temperature. With this information, compute the mean temperature of the liquid. Then, based on the mean liquid temperature, the liquid Reynolds number and Prandtl number are calculated. Using this, the Nusselt number for the liquid is found. Also using the mean liquid temperature property values, the inside heat transfer coefficient is calculated. Based on this inside heat transfer coefficient, a new wall temperature estimate is computed. This procedure is repeated until the T_w converges upon a stable value.

2.4. Frictional loss calculation

The Darcy friction factor for the liquid flow is found using the following correlations from ASHRAE fundamentals [1]:

$$f = 8\left[\left(\frac{8}{Re}\right)^{12} + \frac{1}{(A + B)^{1.5}}\right]^{1/12} \tag{25}$$

where

$$A = \left[2.457\ln\left(\frac{1}{\left(\frac{7}{Re}\right)^{0.9}+\left(\frac{0.27\varepsilon}{d_i}\right)}\right)\right]^{16} \quad \text{and} \quad B = \left(\frac{37{,}530}{Re}\right)^{16}$$

The frictional head loss for liquid flow in a pipe is then computed using the friction factor with the following relation presented by White [17].

$$h_F = \frac{f}{d_i}\frac{LV^2}{2g} \tag{26}$$

This is converted to pressure loss by using the following equation:

$$\Delta P = \rho g h_F \tag{27}$$

The fluid pumping power required per unit length of pipe to overcome this frictional pressure loss is found using the following equation from White [17].

$$\dot{W} = \dot{m}\frac{\Delta P}{\rho} \tag{28}$$

2.5. Thermal resistance calculation

The thermal resistance is a measure of the temperature difference required to drive a given amount of heat flow. For the purpose of this analysis, the thermal resistance to forced convection across the inside boundary between the liquid and the tube is defined as follows:

$$R_i = \frac{1}{h_i} \tag{29}$$

The thermal resistance to natural convection across the outside boundary (between the fins and outer surface of the tube) and the ambient air is defined as follows:

$$R_o = \frac{(T_w - T_\infty)}{q_o''} \tag{30}$$

The total thermal resistance is found using the following relation:

$$R = \frac{1}{h_i\left(\frac{A_i}{A_o}\right)} + \frac{(T_w - T_\infty)}{q_o''} \tag{31}$$

3. Validation of heat transfer model and methodology

Though the method of computing the finned-tube heating capacity is intuitively correct, it is important to validate the model by comparing predicted results with reference data to ensure that the model has been executed properly and that assumptions employed to facilitate the model do not introduce unreasonable errors into the results. Validation of this model is accomplished by comparing data generated by the model to performance rating data for Rittling finned tube from Hydro-Air, Inc. [12] using identical geometry, and inlet conditions for liquid and air.

The configuration of the finned tube that was used to validate the model had the following configuration: tube inside diameter 20 mm (0.785 in), with square fins 108 mm (4.25 in) on a side, on a pitch of 6.4 mm (0.25 in). Ambient air temperature was 291 K (65 °F). Fluid velocity modeled was 0.914 m/s (3 ft/s). The manufacturer's rating data is given with water as the heating medium, and so the model was tested using water. Dimensions for the finned-tube heating unit are shown in Fig. 1.

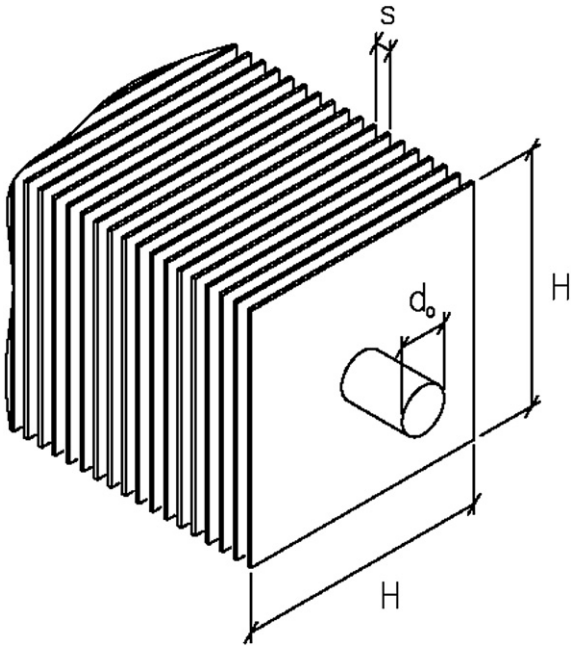

Fig. 1. Finned heating coil configuration.

For these comparisons, the entering water temperature was varied between 372 K (210 °F) and 347 K (165 °F). The Reynolds number for the water range from 65,662 to 44,971. Typically, manufacturers rate finned-tube heating units according to mean water temperature. Data generated by the model was directly compared to the manufacturer's data directly on this basis.

The results of these analyses show that the model agrees reasonably well with the manufacturer's product data. In Fig. 2 the heating capacity data generated by the model is presented next to the manufacturer product data [12].

As shown in Fig. 2, as mean water temperature is varied, the qualitative trend of the model output follows the manufacturer's product data well over the range of temperatures considered. At the lower end of the mean water temperatures considered, the model predicts heating capacity 9.42% higher than the product data [12]. At the high end of the range, the model predicts heating capacity 10.07% higher than the product data. Average absolute deviation is 9.70% over the range of mean water temperatures examined.

In Fig. 3, as average water velocity was varied, once again the qualitative trend of the model output followed the reference data well. The data in this figure is for a finned tube, configured with

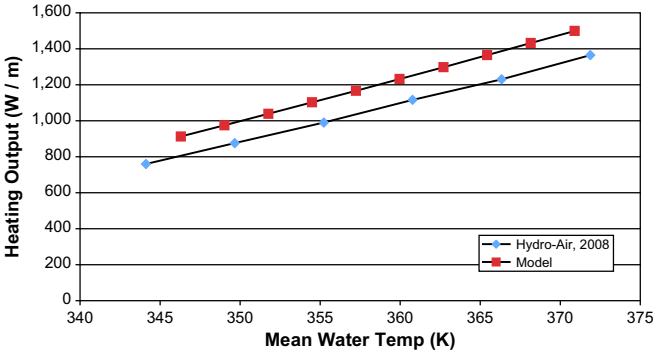

Fig. 2. Finned tube rated heating output versus model predicted capacity, variable mean water temperature.

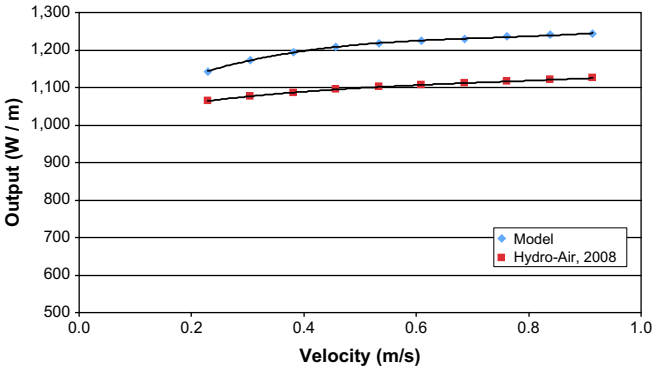

Fig. 3. Finned tube rated heating output versus model predicted capacity, constant average water temperature.

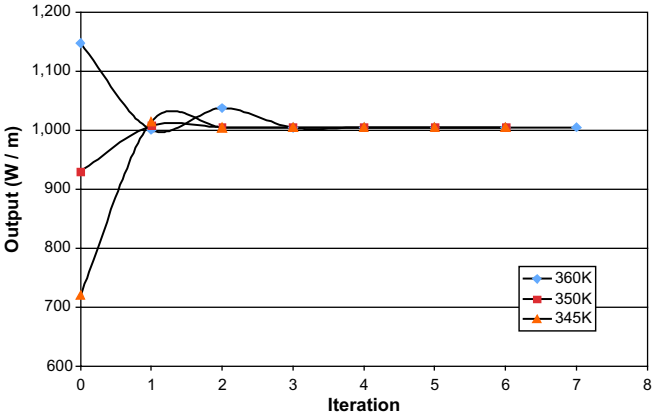

Fig. 4. Convergence of model output as the initial wall temperature guess is varied.

a steel pipe and steel fins. Appropriate dimensions, and material properties for the steel and the steel fins were entered into the model. Once again average absolute deviation is 10% over the range of average water velocities considered. These two validation runs demonstrate that the model consistently predicts output in excess of the unit's rated output, over a wide range of operating parameters.

There are a number of simplifications adopted in the model in order to facilitate use of this computational model that may contribute to deviation from the device's actual performance. The key assumptions are that there is fully turbulent liquid flow inside the tubing at $Re > 3000$, fully developed flow at the inlet of the tubing, and negligible thermal resistance across the thin-walled tubing. Furthermore, the fins as modeled are rectangular. Since the actual fins are stamped from sheet stock, they have radiused tips. The total fin area modeled, therefore, is somewhat higher than that of the actual finned tube, contributing to higher than rated output. The model also assumes that all fins are "thin", meaning heat transfer from the tips is neglected. With a fin density of 158 per meter, and fin thickness of 0.4 mm, this represents 0.8% of the total heat transfer area, so it is reasonable to neglect the heat transfer from the fin tips. A detailed analysis of these errors is not necessary for this paper, as the validation runs indicate that the model captures the qualitative behavior of the finned tube heater quite well. This will allow performance comparisons between heating fluids to be conducted with confidence over a wide range of operating parameters. Admittedly, it is not recommended as a highly accurate model for predicting the performance of a particular type of finned tube.

Sensitivity analyses were conducted to verify that the model was insensitive to the initial guess of wall temperature used in Eq. (24). The iteration routine was executed holding all inputs constant except for the initial guess of wall temperature. The results of the analyses are illustrated graphically in Fig. 4.

The experiment demonstrates that as the initial guess for wall temperature is varied from 345 K to 360 K, the model converges upon the same value after a small number of iterations. This provides evidence that the algorithm developed for this analysis produces output that converges on a single result that is constant as the initial guess varies.

4. Results and discussions

As discussed previously, nanofluids typically exhibit higher thermal conductivity and viscosity than their base fluid; the value of both properties increase with increasing volumetric concentration. In contrast, specific heat decreases moderately with increasing volumetric concentration. The net effect is that Prandtl number increases as nanoparticle volumetric concentration increases. This, in turn, leads to a Nusselt number that also increases with volumetric concentration. The Nusselt number for nanofluids is higher than the base fluid in pipe flow at equal Reynolds number. The increase in Nusselt number, in combination with the higher thermal conductivity has the effect of increasing the convective heat transfer coefficient on the inside of the tube. This has the overall effect of improving heat transfer between the hot liquid and the cooler air by lowering the overall thermal resistance between the two mediums. However, due to the higher viscosity of the nanofluid relative to the base fluid, this enhancement can come with a penalty in pumping energy consumed at equal average liquid velocity. These two competing factors must be weighed against each other to determine the utility of a particular nanofluid as a means of improving heating system performance.

4.1. Finned tube heating performance

It is common in arctic environments (such as northern Alaska) to employ "high temperature" heating systems for HVAC applications in systems that employ finned tube heaters. The mean liquid temperatures across the finned sections in these devices are commonly 350–352 K (170–175 °F). They are usually installed along the exterior walls of occupied rooms, where rates of heat loss to the outside are highest. A zone control valve tied to a zone temperature sensor or thermostatic control will usually cycle open in response to a drop in room temperature, thereby allowing hot fluid to flow through the finned tube section. Heat is delivered to the occupied space by way of natural convection over the heated fins.

For this study, the heating capacity for a finned tube with fixed geometry is modeled with CuO/60% EG and Al_2O_3/60% EG nanofluids and compared to heating capacity with 60% EG. The finned tube geometry modeled is identical to the finned tube used in the model validation runs. Inlet conditions are selected to represent those seen in typical HVAC systems: entering liquid temperature is 383 K (180 °F), and the ambient air temperature is 288 K (60 °F).

4.1.1. Variable fluid velocity finned tube heating output

Fig. 5 illustrates the predicted heating capacity of finned tube with inlet conditions just described. The finned tube is modeled with CuO/60% EG of 1–4% volumetric concentration and the base fluid. Since Xuan and Li's [18] correlation was developed from experimental data on nanofluids with volumetric concentrations up to 2%, the data at 3 and 4% are extrapolated. This is performed for the sake of gaining insight into performance trends of the nanofluids, in the absence of a more appropriate correlation.

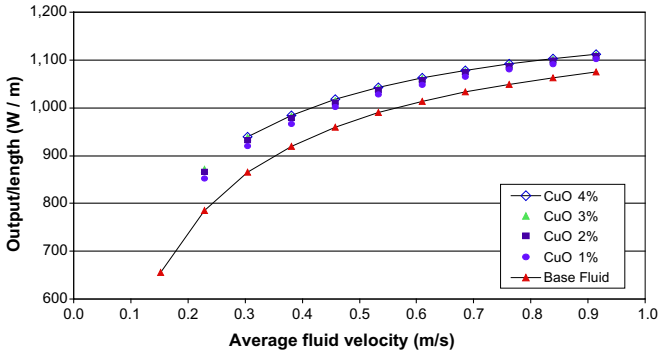

Fig. 5. Finned-tube heating capacity with high temperature CuO nanofluid at variable liquid velocity.

The model predicts higher heating capacity for the finned tube with the CuO/60% EG nanofluid over the range of liquid velocities examined. The 4% volumetric concentration nanofluid has higher output than the nanofluids of lesser concentration, though by a very slim margin. Mean Reynolds numbers for the 4% CuO/60% EG nanofluid ranges from 3506 at 0.305 m/s average liquid velocity to 10,857 at 0.914 m/s average liquid velocity. This equates with volumetric flows of 1.5–4.5 GPM. The finned-tube heating output enhancement is greatest at the lower velocities. The capacity of the 60% EG – filled finned tube approaches that of the nanofluid – filled finned tube as average fluid velocity approaches 1.0 m/s. At an average fluid velocity of 0.305 m/s, the boost in heating capacity is 8.7% with the 4% CuO/60% EG nanofluid as compared to the same finned tube with the base fluid. The improvement in capacity diminishes to 3.4% as average fluid velocity reaches 0.914 m/s. As the average fluid velocity increases, the relative importance of the inside convective heat transfer coefficient in the overall resistance to heat transfer decreases since as the airside convective heat transfer coefficient remains nearly constant with increasing liquid velocity and eventually dominates over the resistance to heat transfer on the inside of the tube.

As with the CuO/60% EG nanofluid, finned-tube heating capacity with the Al_2O_3/60% EG increases relative to the capacity with 60% EG for identical inlet conditions. Fig. 6 illustrates the increased finned-tube heating capacity with nanofluid concentrations up to 4%. The data show that as the volumetric concentration of the Al_2O_3/60% EG nanofluid increases, heating capacity increases proportionally. Reynolds number for the 4% Al_2O_3/60% EG nanofluid ranged from 4499 to 13,931 over the range of average liquid velocities modeled. As seen with the CuO/60% EG nanofluid, finned-tube heating capacity enhancement with the Al_2O_3/60% EG nanofluid is greatest at lower average liquid velocities. As liquid velocity is increased, the heating capacity of the finned tube with the nanofluids approaches that with the base fluid, although not to the extent that exhibited by the finned tube with the CuO/60% EG nanofluid for equal inlet conditions. At an average fluid velocity of 0.305 m/s, the boost in finned-tube heating capacity is 11.6% with the 4% Al_2O_3/60% EG nanofluid compared to heating capacity with the base fluid. As fluid velocity is increased to 0.914 m/s, the difference in heating capacity is only 4.6%.

The thermophysical properties of a nanofluid are affected by the size of the nanoparticles in suspension. The conductivity correlations employed for this analysis predict that as nanoparticle size decreases, thermal conductivity increases. This has the effect of increasing the heating output of the finned tube when other conditions are held constant. As the nanoparticle diameter is decreased from 30 nm to 10 nm for the CuO/60% EG nanofluid, heating output increases by 1.3%. Similarly, as the nanoparticle diameter is decreased from 44 nm to 10 nm for the Al_2O_3/60% EG nanofluid, heating output increases by 1.8%. Unfortunately, the viscosity correlations used for this analysis do not account for the effect of nanoparticle size on viscosity, so the full extent of particle size effects on heating output cannot be fully explored through this analysis.

4.2. Finned tube performance comparison

4.2.1. Liquid frictional pressure loss comparison

Fig. 7 illustrates the relationship between finned-tube heating capacity and liquid frictional pressure loss for the finned tube with 60% EG, and with Al_2O_3/60% EG nanofluid. The graph is created by plotting calculated frictional pressure loss against calculated finned-tube heating output. Heating output is varied by adjusting liquid velocity, while geometry and material properties remain constant. Presenting the performance data in this way illustrates that the Al_2O_3/60% EG nanofluid has lower liquid frictional pressure loss per unit length of pipe, at all concentrations modeled, than the finned tube with 60% EG at a given finned-tube heating output. To allow a quantitative comparison of frictional pressure drop for the base fluid and the nanofluid at a particular heating output, the pressure drop at 1000 W/m is found using interpolation. With 4% Al_2O_3/60% EG nanofluid, the frictional pressure loss at 1000 W/m heating output is approximately 40% less than that required for the finned tube with the base fluid at an equivalent heating output. The difference for the Al_2O_3/60% EG nanofluid at the lower concentrations is 40%, 37%, and 31% at 3%, 2% and 1% volumetric concentrations, respectively. Presenting these data in this way shows a tight grouping for the finned-tube heating output over the range of volumetric concentrations studied. This shows that increased

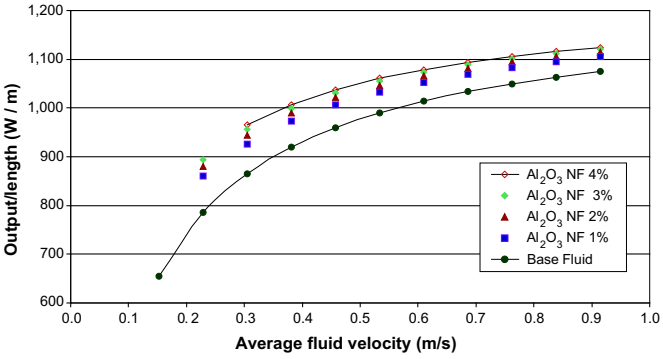

Fig. 6. Finned-tube heating capacity with high temperature Al_2O_3 nanofluid at variable liquid velocity.

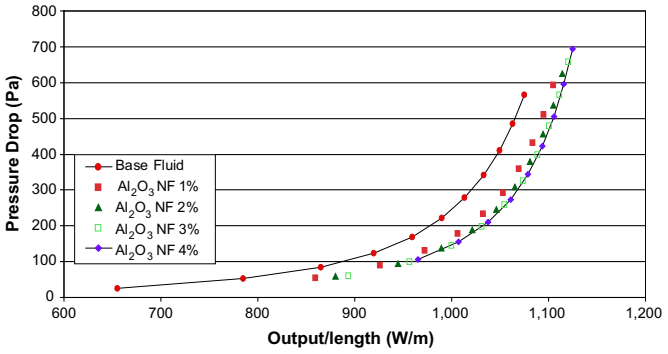

Fig. 7. Finned-tube heating capacity versus liquid friction loss (on a unit length basis) with Al_2O_3 nanofluid and 60% EG.

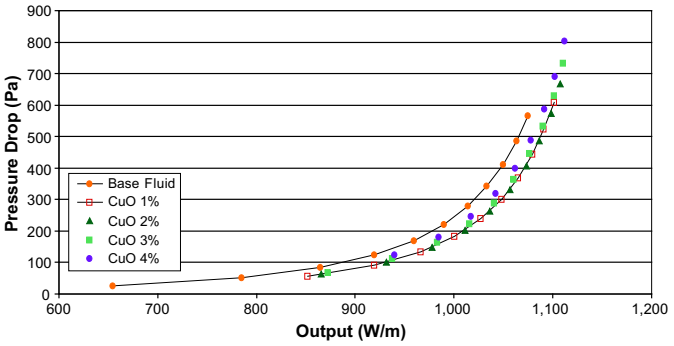

Fig. 8. Finned-tube heating capacity versus liquid friction loss (on a unit length basis) with CuO nanofluid and 60% EG.

heating output associated with higher Al_2O_3/60% EG nanofluid concentration is balanced very closely with increased viscosity contributing to higher frictional pressure loss.

Fig. 8 illustrates the relationship between finned-tube heating capacity and liquid frictional pressure loss for the finned tube with 60% EG, and with CuO/60% EG nanofluid. These data are presented in the same way as described in Fig. 7. With 1% CuO/60% EG nanofluid, the frictional pressure loss was approximately 26% less than that required for the finned tube with the base fluid at an equivalent heating output. The difference for the CuO/60% at the higher concentrations is 25%, 21%, and 14% at 2%, 3% and 4% volumetric concentrations, respectively. The model predicts that the Al_2O_3/60% EG nanofluid thermophysical properties are such that increasing the volumetric concentration results in decreasing pressure loss associated with a given heating output within the range of concentrations examined. In contrast, for the CuO/60% EG nanofluid, it appears that there is an optimal concentration of approximately 1% that minimizes pressure drop.

4.2.2. Liquid pumping power comparison

Fig. 9 depicts a chart of the liquid pumping power required to overcome the frictional pressure drop through the tubing for 4% Al_2O_3/60% EG, 1% CuO/60% EG nanofluids and the base fluid. For a given heating output, the finned tube with the 4% Al_2O_3/60% EG and the 1% CuO/60% EG nanofluid require substantially less pumping power than with the base fluid. For 1000 W/m heating output, the 4% Al_2O_3/60% EG nanofluid requires approximately 61% less pumping power than that required for the finned tube with the base fluid. At the same output, the 1% CuO/60% EG requires approximately 41% less pumping power.

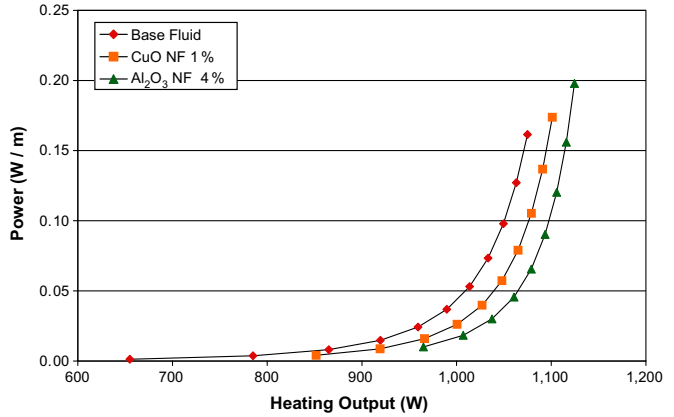

Fig. 9. Liquid pumping power required for a given heating output (on a unit length basis) for finned tube with nanofluids and 60% EG.

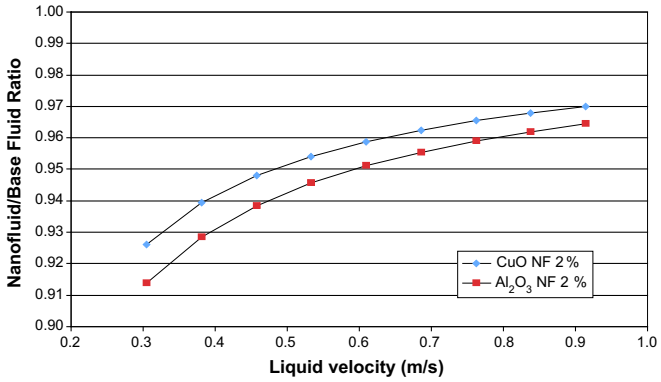

Fig. 10. Total thermal resistance ratio (nanofluid to base fluid) with variable liquid velocity.

4.2.3. Thermal resistance comparison

The analysis indicates that the heat transfer coefficient on the inside of the tube is increased significantly by the use of nanofluids. Accordingly, the thermal resistance to heat transfer is reduced across this boundary. At lower liquid velocities, the inside thermal resistance represents a higher percentage of total thermal resistance, and so the increase in heat transfer coefficient attributable to the use of nanofluids has a proportionally greater affect on finned-tube heating output. For instance, with 60% EG at a liquid velocity of 0.305 m/s, the inside thermal resistance represents 21.8% of the total thermal resistance. In contrast, at a liquid velocity of 0.914 m/s, the inside thermal resistance represents 8.9% of total thermal resistance. For 2% Al_2O_3/60% EG, the total thermal resistance is reduced from 3.6% to 8.6% in comparison to the base fluid as liquid velocity is reduced from 0.914 m/s to 0.305 m/s, respectively. The reduction in total thermal resistance for 2% CuO/60% EG compared to the base fluid is comparable, but not as dramatic. Fig. 10 illustrates the total thermal resistance as a ratio to that for the base fluid over a range of liquid velocities.

4.2.4. Heat transfer area comparison

Fig. 11 illustrates the fin density necessary to facilitate a given rate of heat transfer for given entering fluid conditions for a finned-tube heating unit with 4% Al_2O_3/60% EG and 60% EG. This graph is generated by varying fin density, thereby changing the total heat transfer surface area of the heating unit. The heating capacity is computed by varying fin pitch from 6.35 mm to 11.29 mm (equivalent to fin densities of 2.25–4 fins/inch). The axes are then inverted (the fin pitch is actually the independent variable) in order to more clearly show the effect of the nanofluid on the relationship between fin pitch and heating output.

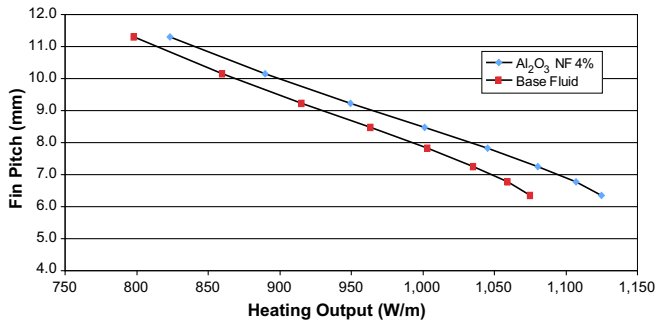

Fig. 11. Comparison of total heat transfer area required for the heating coil for given heating capacities and different fluids.

For these runs, the entering fluid temperature is 355 K, with average velocity of 0.914 m/s (3 ft/s). Tube and fin dimensions are unchanged from before. The graph shows that over the range of heating capacities examined, for a given finned tube heat output, a lower fin density is required with a nanofluid heat transfer medium than the base fluid, assuming identical inlet conditions and finned tube geometry. The finned-tube heating unit with 4% Al_2O_3/60% EG nanofluid requires between 2.8% and 14.5% less fin area, at heating outputs of 750 and 1100 W respectively. This is significant because, for a given finned-tube heating output, less finned area is necessary with nanofluids. As mentioned previously, for a given finned tube configuration, and entering fluid conditions, nanofluids improve the radiator's output. Consequently, for a given heating output the length of finned tube may be reduced in proportion with the increased heating output. Both of these characteristics may be exploited to save materials of construction in a building HVAC system.

5. Conclusions

A model was used to compare finned tube heating performance with 60% ethylene glycol and CuO/60% EG and Al_2O_3/60% EG nanofluid. Entering fluid conditions were typical of those found in commercial heating systems in subarctic and arctic regions. The model predicts that finned-tube heating output with Al_2O_3/60% EG nanofluid is superior compared to that of the heating capacity with CuO/60% EG nanofluid, and of the base fluid. Finned-tube heating capacities with the CuO/60% EG and Al_2O_3/60% EG nanofluid are superior to that with the base fluid at all concentrations examined. For both nanofluids, heating capacity increases with nanoparticle volumetric concentration.

Finned-tube heating capacity was modeled over a range of liquid velocities that are typical of those used in finned-tube heating units. Generally, as average liquid velocity increases, heating capacity with the CuO/60% EG, the Al_2O_3/60% EG and the base fluid increase steadily. In regimes of lower average liquid velocities (and Reynolds number), the deviation between the nanofluids and the base fluid is greater, and the benefits of the nanofluids are more apparent. The model predicts that 4% Al_2O_3/60% EG nanofluid yields a heating output that is 11.6% greater than with the base fluid at 0.305 m/s. The 4% CuO/60% EG nanofluid yields a finned-tube heating output that is 8.7% greater than with the base fluid with the same entering conditions. As velocity increases to 0.914 m/s the difference in heating output decreases to 4.6% and 3.4% greater than that for the finned tube with the base fluid than for the finned tube with the 4% Al_2O_3/60% EG and the 4% CuO/60% EG, respectively.

When compared on the basis of equivalent heating output, the use of these types of nanofluids results in a reduction of pumping power owing to the fact that lower average liquid velocity is required for equal heat output at equal entering conditions. For 4% Al_2O_3/60% EG nanofluid, at a heating output of 1000 W/m the liquid pumping power to overcome the frictional pressure drop is approximately 61% less than that required with the base fluid at the same heating output. For the CuO/60% EG nanofluid, the nanofluid with 1% volumetric concentration has the lowest pumping power requirement of the concentrations modeled. For 1000 W/m heating output, pumping power required for the 1% CuO/60% EG, is 41% less than that required for the finned tube with the base fluid.

The improved heat transfer performance of these nanofluids may also be exploited to reduce the amount of finned area necessary for a given rate of heat transfer at equal flow velocity. When compared at equal heating outputs, a finned tube with 4% Al_2O_3/60% EG requires fin density up to 14.5% lower than that for a finned tube with base fluid. Finned length required for a given output may also be reduced in proportion to the increased output for a given finned tube configuration.

The heat transfer performance of the Al_2O_3/60% EG and the CuO/60% EG nanofluids is superior to that of their corresponding base fluid in this application. These enhanced properties may be exploited to realize a reduction in pumping power, or reduction in the size of heating equipment required to accomplish a given amount of heat transfer. Since the correlations for thermophysical properties employed in these analyses have been developed based on experiments on these specific nanofluids, it is not possible to make general conclusions about the performance of nanofluids in this application.

Appendix. Nomenclature

A	heat transfer surface area (m^2)
C_1	fin geometric parameter
c_p	specific heat (J/kg K)
d_p	particle diameter (m)
d_i	tubing inside diameter (m)
d_o	tubing outside diameter (m)
D_E	effective fin diameter (m)
f	Darcy friction factor
GPM	gallons per minute
g	gravitational acceleration (m/s^2)
h	convective heat transfer coefficient (W/m^2 K)
h_F	frictional head loss (meters of fluid gage)
H	fin height (m)
k	thermal conductivity (W/m K)
L	length (m)
$\dot{m}$	mass flow rate (kg/s)
Nu	Nusselt number (hd_i/k)
ΔP	pressure drop (Pa)
Pe_d	particle Peclet number ($v_{nf}d_p/\alpha_{nf}$)
Pr	Prandtl number ($c_p\mu/k$)
q	total heat transfer rate (W)
q''	heat flux (W/m^2)
R	thermal resistance (m^2 K/W)
Ra	Rayleigh number
Re	Reynolds number ($\rho V d_i/\mu$)
s	fin pitch, fin to fin (m)
T	temperature (K)
$\dot{W}$	pumping power (W)

Greek symbols

α	thermal diffusivity ($k/\rho c_p$)
β	coefficient of volumetric thermal expansion (1/K) in Eq. (14) and a curve-fit constant in Eq. (12)
β_1	geometric parameter
ε	pipe roughness (m)
κ	Boltzmann constant ($1.3806503 \times 10^{-23}$ m^2 kg/s^2 K)
μ	dynamic viscosity (mPa s)
η	fin efficiency
ϕ	volumetric concentration
ρ	density (kg/m^3)
ζ	diameter ratio

Subscripts

i	inside
f	base fluid
m	mean
nf	nanofluid
o	outside
s	solid nanoparticle

References

[1] ASHRAE Handbook Fundamentals Chapter 21, American Society of Heating, Refrigeration and Air Conditioning Engineers, Inc., Atlanta, 2005.
[2] A. Bejan, Heat Transfer Appendix D. John Wiley and Sons, New York, 1993.
[3] J. Buongiorno, Convective transport in nanofluids. Journal of Heat Transfer 128 (2006) 240–250.
[4] J.A. Eastman, S.U.S. Choi, S. Li, W. Yu, L.J. Thompson, Anomolously increased effective thermal conductivities of ethylene glycol based nanofluids containing copper nanoparticles. Applied Physics Letters 78 (6) (2001) 718–720.
[5] V. Gnielinksi, New equations for heat and mass transfer in turbulent pipe and channel flow. International Chemical Engineering 16 (1976) 359–368.
[6] R.L. Hamilton, O.K. Crosser, Thermal conductivity of heterogeneous two-component systems. Industrial and Chemical Engineering 1 (1962) 187–191.
[7] J. Koo, C. Kleinstreuer, A new thermal conductivity model for nanofluids. Journal of Nanoparticle Research 6 (2004) 577–588.
[8] Q. Li, Y. Xuan, Convective heat transfer and flow characteristics of Cu–water. Science in China 45 (4) (2002) 408–416.
[9] P.K. Namburu, D.P. Kulkarni, D. Misra, D.K. Das, Viscosity of copper oxide nanoparticles dispersed in ethylene glycol and water mixture. Experimental Thermal and Fluid Science 32 (2007) 397–402.
[10] B.C. Pak, Y.I. Cho, Hydrodynamic and heat transfer study of dispersed fluids with submicron metallic oxide particles. Experimental Heat Transfer 11 (1998) 151–170.
[11] R.C. Reid, J.M. Prausnitz, T.K. Sherwood, The Properties of Gases and Liquids, fourth ed. McGraw Hill, New York, 1987.
[12] Rittling Finned Tube Product Catalog. Hydro-Air Components, Inc, New York, 2008, pp. 4–6.
[13] G.D. Raithby, K.G.T. Hollands, Natural convection Chapter 4. in: W.M. Rohsenow, J.P. Hartnett, Y.I. Cho (Eds.), Handbook of Heat Transfer. McGraw-Hill, New York, 1998.
[14] R. Vajjha, Measurement of Thermophysical Properties of Nanofluids and Computation of Heat Transfer Characteristics, M.S. thesis, University of Alaaska Fairbanks, 2008, 150 pp.
[15] R. Vajjha, D.K. Das, Experimental determination of thermal conductivity of three nanofluids and development of new correlations. International Journal of Heat and Mass Transfer (2009). doi:10.1016/j.ijheatmasstransfer.2009.06.027.
[16] R. Vajjha, D.K. Das, Specific heat measurement of three nanofluids and development of new correlations. Journal of Heat Transfer 131 (2009). doi:10.1115/1.3090813 7pp., ASME, New York.
[17] F.M. White, Viscous Fluid Flow, second ed. McGraw Hill, New York, 1991.
[18] Y. Xuan, Q. Li, Investigation of convective heat transfer and flow features of nanofluids. Journal of Heat Transfer 125 (2003) 151–155.